Dragline Bucket Carry Angle Control

Peter Ridley
School of Mechanical Engineering,
Queensland University of Technology,
GPO Box 2434,Brisbane 4001, Australia,
(p.ridley@qut.edu.au)

Rindert Algra
Mechanical Engineering
Systems and Control Group,
Delft University of Technology,
Mekelweg 2,2628 CD Delft,
The Netherlands
(d.m.c.vanvondelen@wbmt.tudelft.nl)

Abstract

[1]

This paper examines the automation of dragline bucket excavators used to strip over-burden from open cut mines. The in-plane, open loop system dynamics of a 1:20 scale model dragline bucket are identified and a strategy for automatic control of bucket carry angle and trajectory is presented. Simulated closed loop behaviour of the final system is then validated against experimental results.

1 Introduction

Draglines (Figure 1) are the largest pick and place robots in existence. Using booms of 100 meres length, they strip over-burden from open cut coal mines 120 tonnes at a time.

Incentive to automate the dragline comes from the possibility of increased productivity over manual operation. An additional benefit which may also flow, is the reduction in maintenance costs due to control of peak overloads. Such overloads arise from careless manual operation of the machine, often due to driver fatigue over long shifts.

Considerable success has already been achieved by Winstanely et al [1] in automating the swing axis. The aim of this paper is to investigate the possibility of automating the drag axis.

Productivity of excavation operations is determined by many factors. One important factor is the ability to fill the bucket to maximum capacity and to retain the load without spillage whilst it is being lifted and slewed toward the dump zone.

Howarth et al [2] advise that when a bucket is dragged up the embankment, it fills to a stable shape dependent on drag angle. Bucket capacity is maximised if the lift occurs at the point of intersection on the slope where the carry angle curve and drag angle are equal.

Anecdotal evidence also suggests that care needs to be taken in handling the bucket after break-out. Excess jerk and oscillation causes material to fall from the load from either the front or rear of the bucket. Lifting the load along a line of constant carry angle is another measure which ensures that the load remains intact.

Automatic control of the drag axis can be achieved by measuring bucket carry angle and using this signal in a feedback loop which regulates the payout of the drag-rope. The aim is to dampen bucket oscillation as well as to provide accurate path control along a line of constant carry angle.

Figure 2 shows a typical rigging layout with the bucket carry angle designated (γ). Ridley and Corke [2] and Knights and Shanks [3] describe how the static pose of the bucket/rigging may be determined throughout dragline work-space.

Contours of constant carry angle are identified and are reproduced from [2] in Figure 5. Bucket pose is determined not only by rigging geometry, but also by the payload size and the location of its centre of gravity. These parameters vary with each new load of overburden, hence the curves in Figure 5 are only indicative.

This paper describes the implementation of automatic control of carry angle on a planar scale model manufactured to one twentieth dimensional scale of the full-size machine discussed by Knights and Shanks [3]. Investigation of the bucket/rigging dynamics is presented along with an explanation of a controller design and closed loop responses.

2 Open-loop response

Layout of experimental apparatus and the control-system block diagram are shown in Figures 3 and 4. Investigation of the plant dynamics was carried out by applying a swept sine voltage (V_m) to the drive-motor amplifier and measuring the response (V_g) from the rate-gyro on the bucket. Frequency response was measured using a dual channel spectrum analyser for three different bucket positions (high, mid, low) in the workspace for a single bucket carry angle, zero degrees.

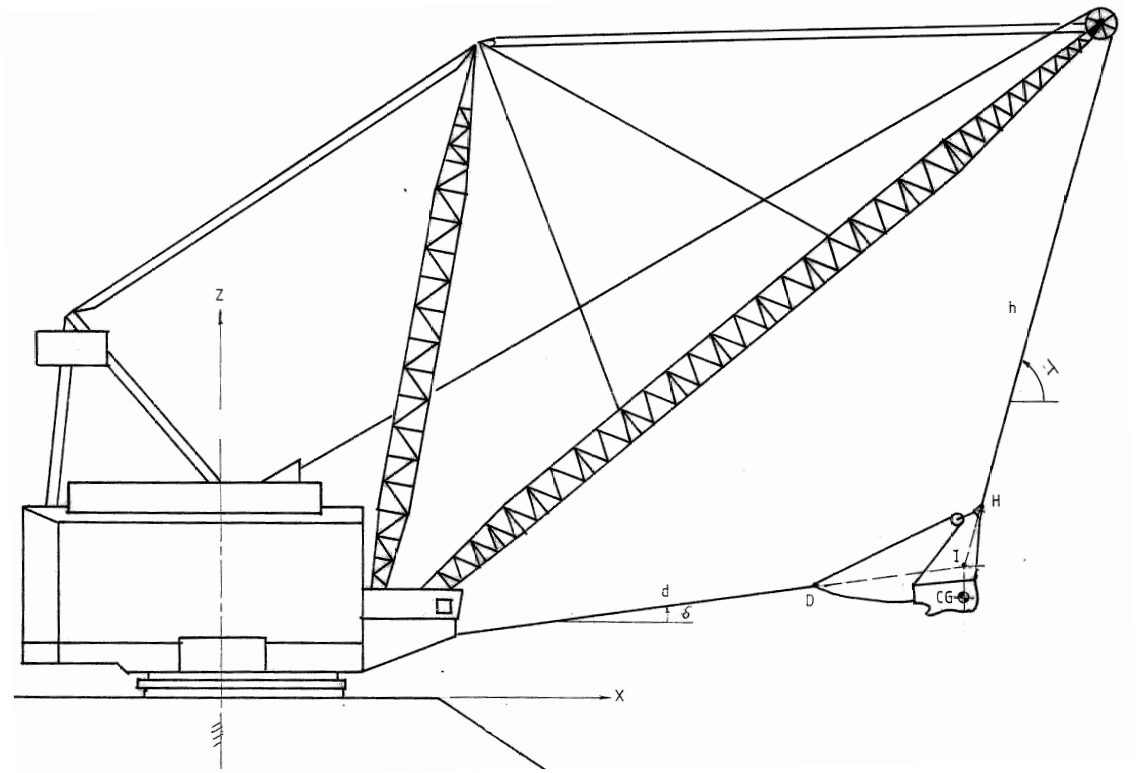

Figure 1: Dragline

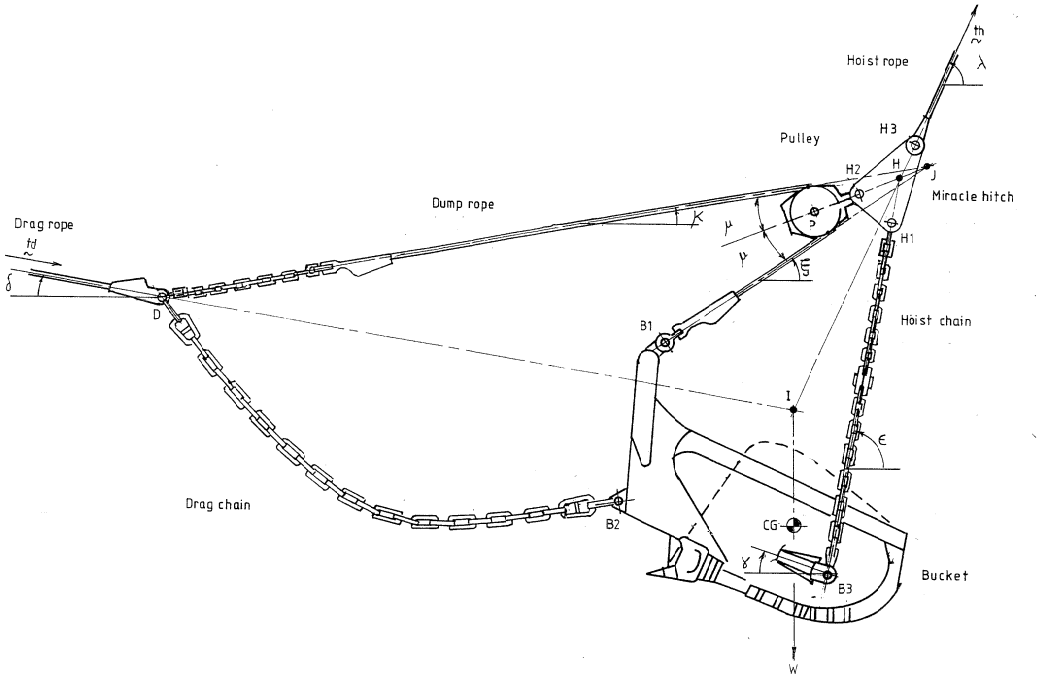

Figure 2: Bucket rigging

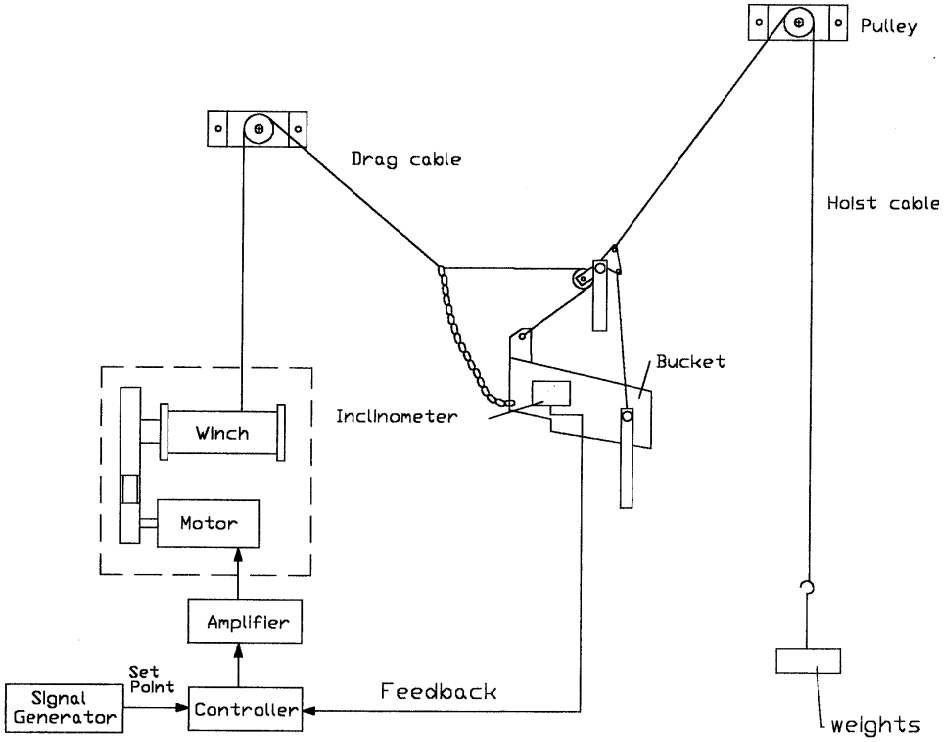

Figure 3: Experimental apparatus

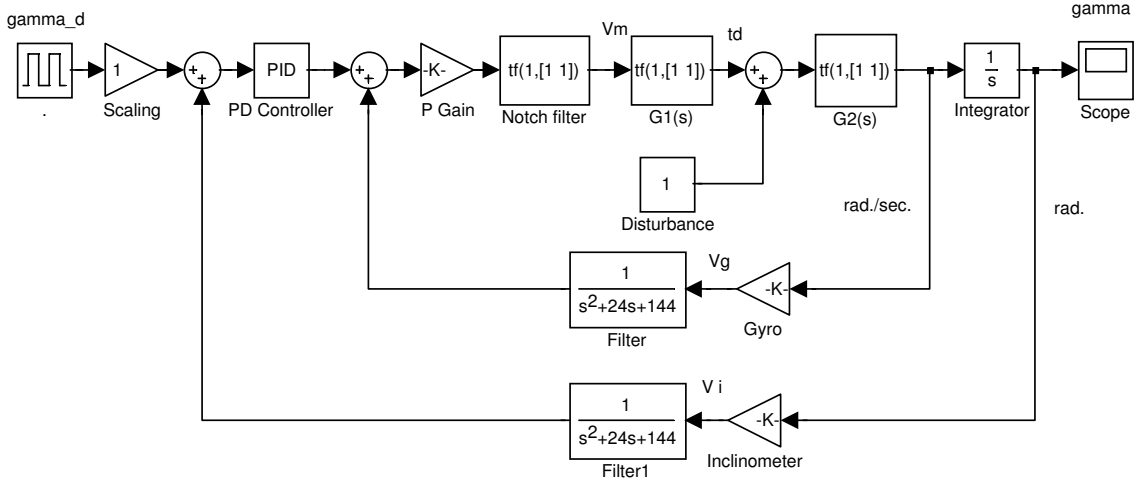

Figure 4: Control loop block diagram

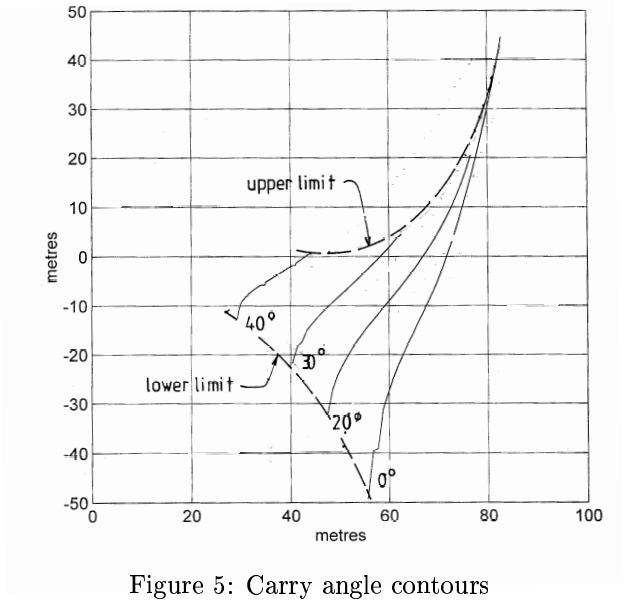

Figure 5: Carry angle contours

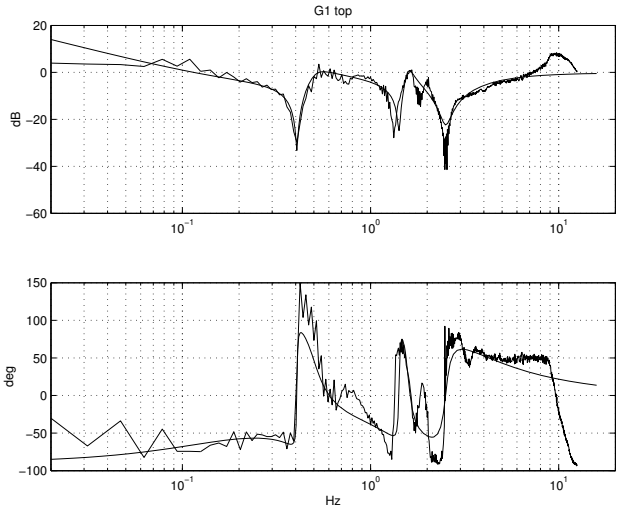

Figure 6: Open loop response ($\frac{t_d}{V_m}$)

The open loop response of the bucket was subdivided into two transfer functions. $G_1(s)$ is transfer function between the voltage input V_m to the amplifier and the tension t_d in the drag rope. $G_2(s)$ is the transfer function between the force t_d in the drag rope and the angular velocity $\dot{\gamma}$ of the bucket. Figures 6,7 and 8 show the experimental and fitted frequency responses for 0 degree bucket carry angle at the top of the dragline workspace. Similar measurents were taken in the middle and low regions of the workspace.

Figure 6 shows three distinct anti-resonances, which are partially cancelled by matching resonant peaks shown in Figure 7. Evidence of this cancellation is shown in Figure 8. The three resonances relate to clearly identifiable pendulum modes of oscillation exhibited by the bucket and rigging. The lowest frequency mode is a simple pendulum mode, wheras the second ("rocking') and third ("pitching") modes are compound pendulum oscillations.

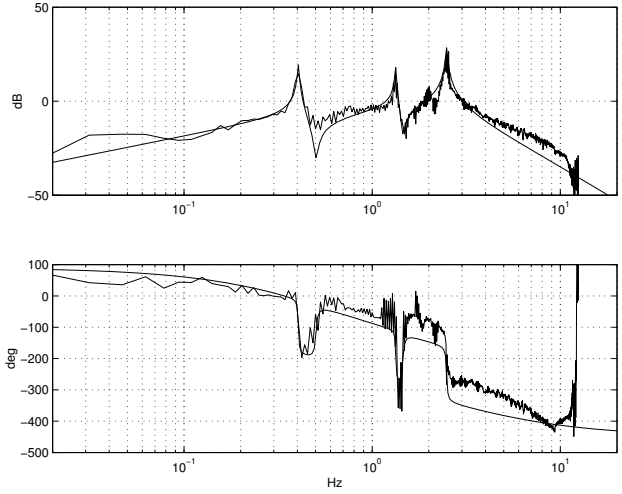

Figure 7: Open loop response ($\frac{\dot{\gamma}}{t_r}$)

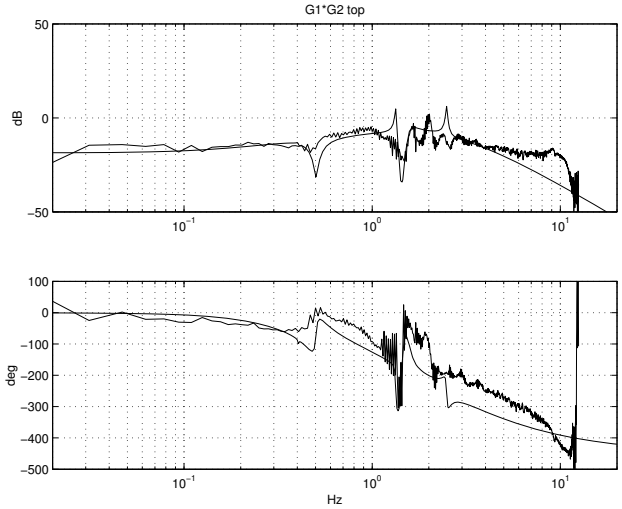

Figure 8: Open loop response ($\frac{\dot{\gamma}}{V_m}$)

Figure 7 also shows a rapid loss of phase which indicates that the system has non-minimum phase behaviour. On the application of a positive voltage (ie reeling inwards) to the drag motor, there is an initial tendency for the bucket to accelerate downwards prior to recovery. Non minimum phase behaviour is associated with zeroes in the right-hand side of the S-plane of transfer function $G_2(s)$.

Zeroes $G_1(s)$	Poles $G_1(s)$
-0.8445 $\pm$ 15.7381i	0
-0.1050 $\pm$ 8.9020i	-12.3478 $\pm$ 8.7112i
-0.0204 $\pm$ 2.5500i	-0.5112 $\pm$ 9.9032i
-1.0953	-0.5317 $\pm$ 3.0756i

Zeroes $G_2(s)$	Poles $G_2(s)$
0	-27.1
-0.1420 $\pm$ 9.1359i	-0.1417 $\pm$ 15.6216i
3.4251	-8.9927
-0.0521 $\pm$ 3.1558i	-0.0630 $\pm$ 8.3805i
	-2.5659
	-0.0204 $\pm$ 2.5459i

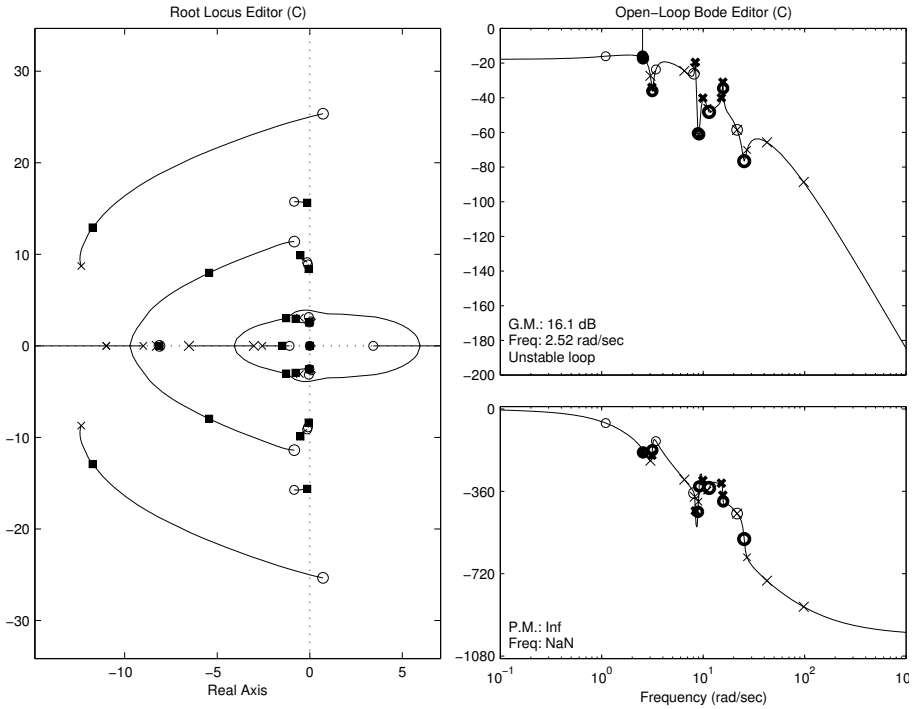

Figure 9: Rate loop : root locus and frequency response diagrams.

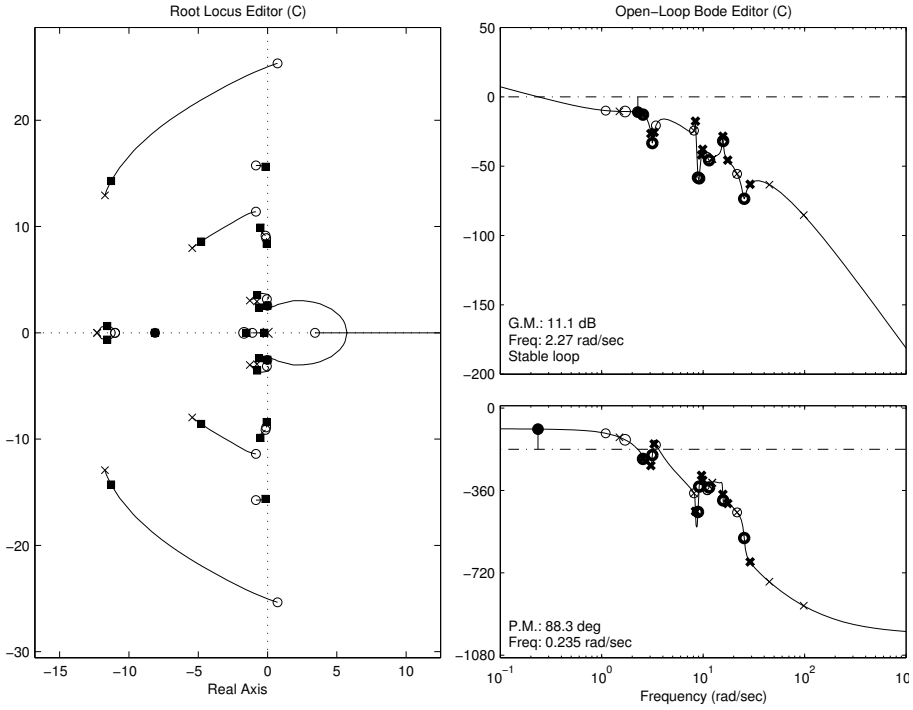

Figure 10: Position loop: root locus and frequency response diagrams.

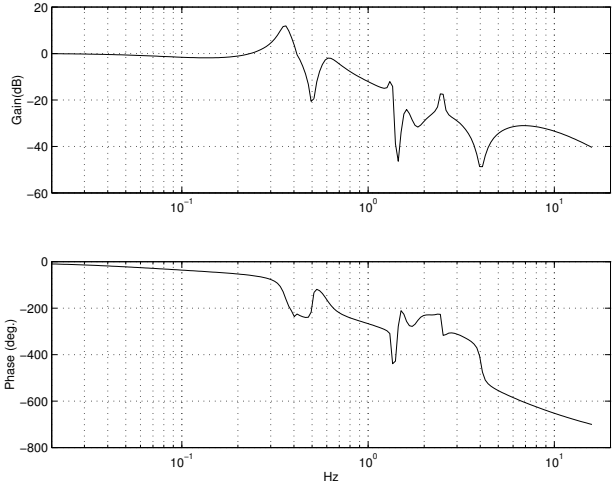

Figure 11: Position closed loop response ($\frac{\gamma}{\gamma_d}$)

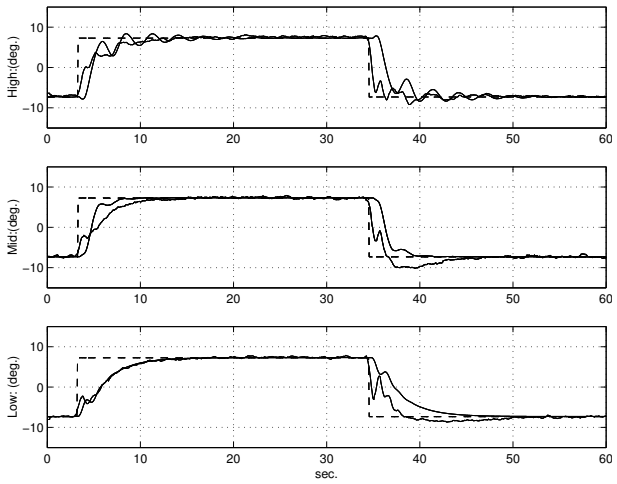

Figure 12: Carry angle step responses: Simulated and Experimental

3 Closed loop response

Rate loop

An inner, rate control loop was created using a gyroscope as the feedback transducer. This inner loop has the beneficial effect of forcing the system to behave in a more linear fashion than the open loop dynamics would otherwise allow.

The controller design is based on the necessity to roll off the system gain before the phase deteriorates. This ensures closed loop stability and was achieved using proportional control combined with notch filters at 1.8 Hz and 6.5 Hz. A double pole filter with a cut off at 1.8 Hz was also included in the rate feedback loop.

Figure 9 shows the root locus for variation of the rate loop's proportional gain. For the chosen proportional gain, all of the closed loop poles lie safely in the left hand side of the S-plane. The bandwidth of inner loop when it is closed is approximately 1.0 Hz.

Position loop

The outer position control loop was compensated using PD control. Root locus and open loop frequency response diagrams shown in Figure 10, show that for the chosen proprtional and derivative gains, the closed loop poles all lie in the left hand plane.

Closed loop frequency response ($\frac{\gamma}{\gamma_d}$) is predicted in Figure 11. System bandwidth is approximtely 0.4 Hz. A resonant peak is also evident at 0.35 Hz but the response falls away rapidly beyond this frequency.

Step inputs of carry angle (γ_d) were applied to the system. Typical responses (γ) for the top of the workspace are plotted in Figure 12. The discrepancies between the predicted and actual response can most likely be attributed to the non-linear nature of the system.

Time responses of carry angle (γ) to disturbance inputs were also measured. Two types of disturbance were applied:

- impulsive hoist rope disturbance,
- impulsive bucket disturbance.

Both sets of disturbance result in the bucket angle returning to its set carry angle, with negligible residual error in a settling time of approximately 5 to 6 seconds.

A test was also conducted where the bucket was slowly raised from a position low in the workspace to high in the workspace and then returned. It automatically traveled along the constant bucket angle contour trajectory described in Figure 5.

4 Conclusion

Controlling the in-plane motion of a dragline bucket through automatic control of carry angle has proven to be successful. Closed loop responses are stable with an acceptably small steady state error and settling time.

5 Acknowledgements

The authors wish to acknowledge the assistance given to the project by CSIRO Manufacturing Science & Technology, Automation Group , the Australian Coal Research Program for continuing research funding grant C11043 and also Prof. Ton van der Weiden from the Mechanical Engineering Systems and Control Group,Delft University of Technology.

6 References

[1] Winstanley G.J., Corke P.I., Roberts J.M. 1997, Dragline swing automation. IEEE International Conference on Robotics and Automation V3 1997.

[2] Ridley P.R., Corke P.I., 2000, Calculation of dragline bucket pose under gravity loading, Mechanism and Machine Theory, 35 (2000), pp1431-1444

[3] Knights P., Shanks D., 1992 Bucket Rigging influence on dragline productivity, Australian Coal Journal No. 36 1992.

[4] Howarth D.F., Just G.D. , Runge G.A., 1987, Dragline bucket filling characteristics Trans. Inst Min. Metall. (Sect. A Mining Industry), 96, pp 189-192